Mechanism and Analytical Models for the Gas Distribution on the SiC Foam Monolithic Tray

Hong Li
School of Chemical Engineering and Technology, Tianjin University, Tianjin 300072, China

National Engineering Research Center of Distillation Technology, Tianjin 300072, China

Long Fu
School of Chemical Engineering and Technology, Tianjin University, Tianjin 300072, China

Xingang Li
School of Chemical Engineering and Technology, Tianjin University, Tianjin 300072, China

National Engineering Research Center of Distillation Technology, Tianjin 300072, China

Collaborative Innovation Center of Chemical Science and Engineering (Tianjin), Tianjin 300072, China

Xin Gao
School of Chemical Engineering and Technology, Tianjin University, Tianjin 300072, China

National Engineering Research Center of Distillation Technology, Tianjin 300072, China

DOI 10.1002/aic.14944
Published online July 18, 2015 in Wiley Online Library (wileyonlinelibrary.com)

Silicon carbide (SiC) foam material has been applied as monolithic tray for distillation column in our previous study. A systematic understanding of the gas distribution process on the foam tray should help to the design of commercial application. In this article, local gas holdup distribution and bubble size distribution are used to measure the gas distribution. The local gas holdup is tested by the conductive probe and the number of test point is counted in different local gas holdup. The bubbles are captured by the high-speed camera to measure the bubble size. Bubble size is calculated as ellipsoidal bubble and counted with different pore sizes. Furthermore, a three-stage process model is put forward to explain the uneven distribution of gas phase, and verified by the experimental values. The results show that the structure and the thickness of SiC foam is the decisive factor for the gas distribution performance. © 2015 American Institute of Chemical Engineers *AIChE J*, 61: 4509–4516, 2015

Keywords: silicon carbide foam monolithic tray, gas distribution, process model, bubble

Introduction

Plate columns are important equipment for mass transfer between gas-liquid and liquid-liquid, because of its simple structure, convenience and stable operation, and low cost.[1] Compared with the packing columns, the plate columns perform better at higher operation pressure. So the study of the new column trays is always the focus of much research. In 2012, Zarei introduced a new type of cap trays called Conical Cap tray,[2] which has good turndown ratio without having too much pressure drop. Union Carbide developed Expansion Capacity Multi-downcomer (ECMD) sieve trays,[3] which particularly perform well in high pressure and high liquid-gas ratio.

In the last few years, the foam Silicon Carbide (SiC) materials have been applied in many fields with low density, good thermal stability, high porosity, and specific area.[4–7] Also the foam SiC material is used in distillation columns, such as SiC packing,[8,9] SiC valve tray,[10] and SiC foam monolithic tray.[11,12] The foam SiC ceramic has wide material sources and low manufacture cost, compared with the metal material, the preparation process of foam SiC ceramic is more environmentally friendly. Therefore, the SiC foam monolithic tray has a better economic and environmental benefits compared with traditional metal internals.[13–15]

The previous study found that the SiC foam monolithic tray had the advantage of lower pressure drop, less entrainment, less weeping, and higher mass-transfer efficiency.[1] The results shown that the SiC ceramic foam tray is an appropriate mass-transfer unit element for a distillation column. However, the applications would be limited to the clean services due to the small orifice size on the tray deck. In additional, the gas-phase distribution in the foam monolithic tray is uneven at the low *F*-factor. Furthermore, the Foam monolithic tray may appear to have a poor mass-transfer performance at the low *F*-factor.

Correspondence concerning this article should be addressed to X. Gao at gaoxin@tju.edu.cn

Therefore, to find out the reasons for the poor distribution of gas phase in the foam tray is crucial to improve the performance of SiC foam trays.

Two factors may influence the gas distribution performance, the local gas holdup distribution and the bubble size distribution. A variety of technologies have been designed to measure the bubble size and the gas holdup, which are classified into two categories[16] invasive and noninvasive. Noninvasive technologies include particle image velocimetry[17] and high-speed camera,[18] which can obtain the bubble data at low-disturbance conditions. Invasive techniques such as flying optical probe[19] and conductive probe[20,21] are suited to industrial-type applications having high-gas holdup.

In this article, we explore the influence of SiC structure to the gas distribution. To reveal the surface structure of SiC foam monolithic tray, x-ray three-dimensional (3-D) imaging technique is used to reconstruct the SiC foam, which is widely used to study liquid flow distribution in packing and porous media. X-ray 3-D imaging technique can faithfully measure 3-D internal structure of SiC foam. Furthermore, we put forward a process model of gas distribution on SiC monolithic foam tray to explain the uneven distribution of gas phase. Two methods are used to study the gas distribution on the SiC foam tray in air-water system. First, we discuss the three-step model to describe the process of gas distribution on SiC foam. Then we use dual conductivity probe to measure the radical profile of local gas holdup, and study the formation mechanism of bubbles on SiC foam tray. The high-speed camera is used to display the bubble size distribution.

Experimental Equipment and Procedure

Structure of SiC foam tray

The material preparation method was developed by the Institute of Metal Research, Chinese Academy of Sciences,[1] which was based on the impregnation of the polyurethane foam with a homogeneous mixture of silicon, charcoal, and phenolic resin. The foam has a surface area between 2200 and 3800 m^2/m^3, an apparent density between 720 and 810 kg/m^3. The SiC foam monolithic trays in the test are squares with 10-cm side length, and different thickness. The foam elements have constant porosity arranged from 61 to 63%. The specific parameters are shown in Table 1.

Experimental setup and procedure

The equipment of experiment is shown in Figure 1. The tests are carried out in the rectangular Polymethyl Methacrylate (PMMA) tower. The tested SiC monolithic foam tray is pasted on the frame of PMMA tower. The experiments are carried out in the air-water system at room temperature and ambient pressure. In the test, the prestore tank filled with water, the water flow over the weir and drop into the downcomer, passing through the test tray and drawing down. Air is sent into the bottom of equipment, distributed homogeneously and flowing through the test tray and liquid layer. U-tube manometer is used to measure the pressure drop of SiC foam tray.

The local gas holdup is obtained by the dual conductivity probe as shown in Figure 1b. In the test, the conductivity probe is dropped into the liquid layer on the test point. When the bubbles pass through the probe, the instrument will detect the changes of conductivity and record the voltage variation, then the local gas holdup can be calculated as Eq. 1

Table 1. Detail Parameters of SiC Foam Monolithic Trays

Thickness (mm)	Pore size (mm)	Porosity (%)
4	2	61
8	2	61
12	2	61
4	3	62
8	3	62
12	3	62
4	4	63
8	4	63
12	4	63

$$\varepsilon_i = \frac{\sum W_{tj}}{t} \tag{1}$$

The local gas holdup (ε_i) is equal to the time of bubbles though the probe ($\sum W_{tj}$) divided by the total testing time (t). Zhang et al.[20,21] assumed that the average gas holdup on the section measured by the conductivity probe is agreed with that measured by pressure drop methods. The standard deviations of the two methods are both less than 8%.[20,21] To measure the local gas holdup as precisely as possible, the test tray is divided into 100 grids for 10×10 cm^2 areas, each grid acts as a test point to measure the local gas holdup. In the experiment, the measuring height of 10 mm on each test point is a fixed value. The test is developed with data acquisition time of 60 s and data acquisition frequency of 1000 Hz. To present the distribution of local gas hold in different points, we count the number of test point at different gas holdup. The tests are carried out on the condition of $F = 1.0\ kg^{1/2} \cdot m^{-1/2} \cdot s^{-1}$, $L = 2.86\ m^2 \cdot h^{-1}$, $H_w = 22$ mm, where F stands the F-factor, L is liquid flow rate, and H_w is the height of overflow weir.

The high-speed camera is used to capture the bubbles, which is provided by Olympus Corporation fall. The high-speed camera is set in the front of test plate, and the visualization of bubble is realized at a rate of 1000 images per second with a size of 1280×1024 pixels. The light source is provided by an indirect 500-W halogen which enlightened the column via a parchment paper between the column and the light source. The bubble size is measured using image analysis software Image Pro Plus (Media Cybernetics Cooperation).[22] Images acquired by the high-speed camera are first converted to gray scale to get a clear bubble boundary. In the present test, the test bubble is equal to an ellipsoidal bubble, and an equivalent bubble diameter is calculated as mean diameter along different axes of bubble. To obtain more comprehensive and accurate data, about 300–500 bubbles are measured for representative bubble size distribution.[23,24]

The high-speed camera has the advantage of visualizing the bubble motion instantly and noninterference flow field. But it has the limitation that the camera neither acquires all the bubbles in the cross section, nor gets bubble boundary clearly at disrupted flow field. In order to calculate the bubble size above the SiC foam tray, one bubbling point is picked and measured. In the test, we assume the all the bubbling points are noninterference each other and the picked one is representative. A plate with only one hole in the center is placed under the test tray. The gas flow through the orifice of glass and the SiC foam tray in sequence. The diameter of the orifice is 4 mm, the gas volume flux is 2.7 m^3/h, the volume flux of the water is 400 L/h, and the down weir is 6 cm height.

In order to measure the bubble size distribution, the total number of bubbles N is divided into m internals from small to large. Therefore, in internal i, the number of bubbles whose diameter is d_i is n_i, the probability density distribution is:

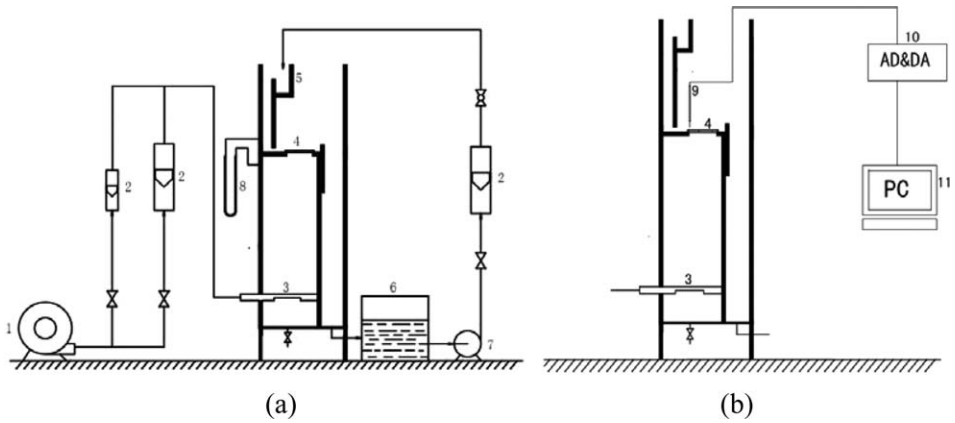

Figure 1. Schematic drawing of experimental setup for the bubble size distribution (a) and the gas holdup distribution (b).

1. Air blower; 2. rotameter; 3. gas distributor; 4. test tray; 5. prestore tank; 6. water storage tank; 7. centrifugal pump; 8. u-tube manometer; 9. probe; 10. transmitter; and 11. Computer.

$$f(d_i)=n_i/N \tag{2}$$

Development of the Process Model

The growth process of bubble from a single orifice was modeled by Kasimsetty,[25] the model represented a balance of buoyance, viscosity, surface tension, liquid inertia, and gas momentum force. The behavior of bubble was described as three steps, incipience, growth, necking, and departure.

From the single orifice theory, we can deduce the single bubble formation on the SiC foam tray. Similarly the history of bubble formation on the SiC foam tray also can be divided into three steps. First is the incipience stage, the gas accumulate in the cavity of the SiC foam until the gas pressure reach the critical pressure which is the minimum value for the bubble formation, the critical pressure includes the hydrostatic pressure, the capillary pressure, and the surface adhesive forces caused by the good wettability of the SiC foam material. When gas pressure reaches critical pressure, the bubbling point can take shape. Second is the growth stage, the bubble expands quickly and takes shape. Third is the necking and departure, the neck of bubble gets cut off and the bubble rises up. In the process of bubble formation on the SiC monolithic foam tray, the forces governing the balance of bubble formation include buoyance, viscosity, surface tension, liquid inertia, and gas momentum force.

Our study starts on the incipience stage. The deciding factor of gas distribution is the distribution of bubbling points, and the bubbling points are the positions where the bubbles take form and grow up. Because the radical distribution of bubbling points is determined in the stage of incipience.

The process of single bubble formation is discussed above. To describe the process of bubble distribution on the SiC foam tray, we put forward a three-stage process model. The process model divides the bubble distribution into three stages. Figure 2 shows the condition of three stages briefly, Figure 2a, b, and c presents the Stages I, II, and III, respectively

$$\text{I.}\quad \begin{cases} d < I_\sigma, P=\rho g h + P_c \\ d > I_\sigma, P=\rho g h + P_\tau \end{cases} \tag{3}$$

The first stage is used to describe the critical condition of bubble formation. In this stage, no gas phase flows through the SiC foam, the pressure under the tray (P) acts the role of momentum force. In the test, the height of liquid layer is

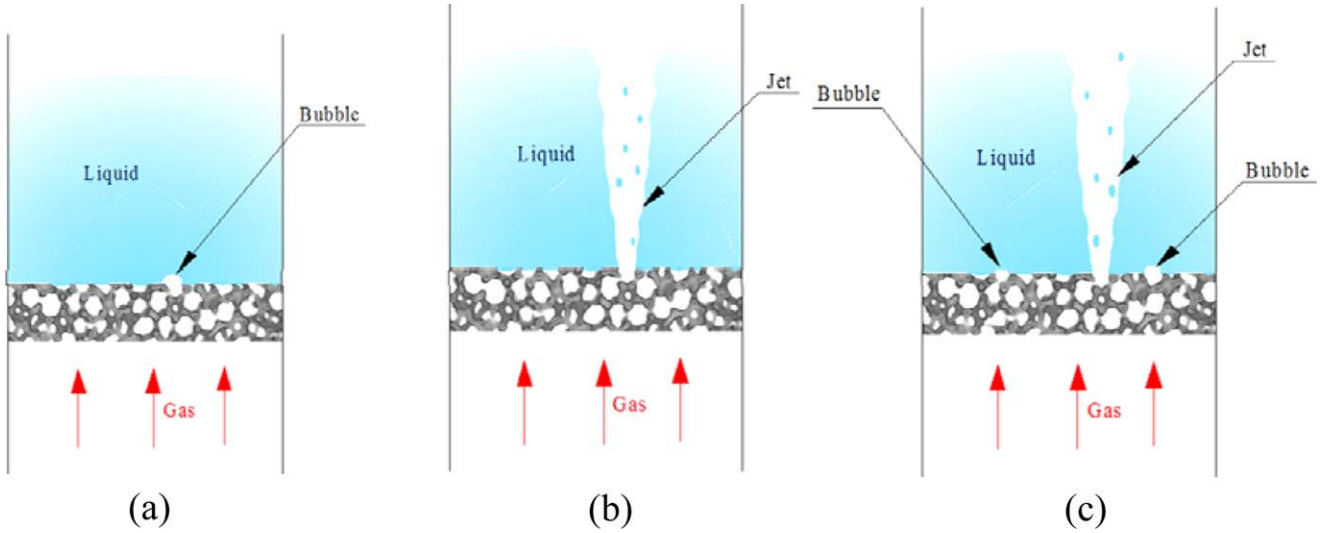

Figure 2. Schematic drawing of the process model for the gas distribution on the SiC foam monolithic tray.

[Color figure can be viewed in the online issue, which is available at wileyonlinelibrary.com.]

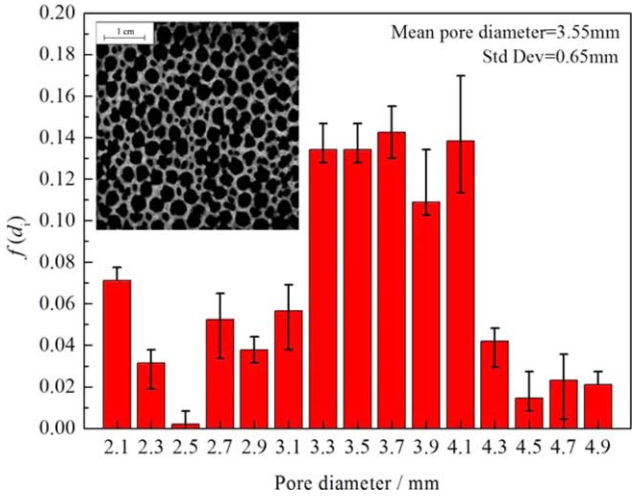

Figure 3. The pore size distribution and the actually structure of the SiC foam monolithic tray acquired by x-ray 3-D imaging techniques.

[Color figure can be viewed in the online issue, which is available at wileyonlinelibrary.com.]

constant, so the hydrostatic pressure (ρgh) is constant. Capillary pressure (P_c) is defined as

$$P_c = 4.08\frac{\sigma\cos\theta}{d} \tag{4}$$

which is decided by the surface tension (σ), contract angle (θ), and the pore diameter (d), acts the role of resistance force. P_τ is defined to describe the resistance force obstructing the air pushing the water in the porous media, which is caused by the surface adhesive force. The surface adhesive force can be described by the contact angle, which is decided by the properties of liquid and wall roughness of SiC.[26]

Capillary length (I_σ) is used to give a measure for the surface tension force. A free surface that has a characteristic length longer than the capillary length can be considered that the system is relatively unaffected by surface tension effects, on the contrary, surface tension dominates. Capillary length is defined as

$$I_\sigma = \left(\frac{\sigma}{\rho g}\right)^{1/2} \tag{5}$$

where σ is the surface tension, ρ is the fluid density, and g is the gravitational acceleration. On the SiC foam tray, the pore size which is less than the capillary length will keep the surface system stable and prevent the liquid invading into the porous of SiC foam. Therefore, when the pore size $d < I_\sigma$, surface tension could keep the gas-liquid surface stable, the capillary pressure (P_c) is the main resistance force; when the pore size $d > I_\sigma$, the gas-liquid surface cannot keep stable, liquid will invade into the porous of SiC foam and obstruct the gas channel, then the gas must push obstructive liquid, overcome surface adhesive force (P_τ)

$$\text{II.}\quad P = \rho gh + \Delta P_{SiC} \tag{6}$$

The second stage describes the quasisteady stage. In this stage, the gas volume flux is stable, the bubbling points have taken shape in the first stage, and there is not new bubbling point taking form in the second stage. Therefore, P_c and P_τ discussed in the first is not under consideration in this stage. ΔP_{SiC} is the pressure drop on SiC foam caused by the gas flow through the tray, and ΔP_{SiC} decides the value of pressure under the tray (P)

$$\text{III.}\quad \begin{cases} d < I_\sigma, \Delta P_{SiC} > \rho gh + P_c \\ d > I_\sigma, \Delta P_{SiC} > \rho gh + P_\tau \end{cases} \tag{7}$$

The third stage is derived from the second stage. The model of this stage is used to describe the positions where no bubble forms in the first stage. In this stage, the requirement for bubble formation is similar to the first stage, only when the pressure under the tray (P) must overcome the resistance force (P_c and P_τ) could the bubbles take form. However, the condition in this stage is not same to the first stage, the pressure under the tray (P) is decided by ΔP_{SiC}, therefore, we can deduce that when the ΔP_{SiC} is larger than the resistance force (P_c and P_τ), the bubbles could take form.

In air-water system, the surface tension of water is σ=72.75 $mN \cdot m^{-1}$, and the capillary length is $I_\sigma = 2.71$ mm. Therefore, we can deduce that, on the SiC tray with 2-mm pore size, the surface tension force can hold up the air-water surface and prevent the water into interspace of SiC foam. On the SiC tray with 4-mm pore size, the pore diameter is larger than the capillary length, thus the surface cannot keep the air-water surface and water can attach into the interspace. On the SiC tray with 3-mm pore size, the pore diameter stands near the capillary length, which means that some of surface hole diameter may be larger than the capillary length but some smaller. Therefore, the surface tension force act the role of preventing water in some positions of SiC foam tray. In summary, the pore diameter decides the resistance pressure drop (P_c and P_τ) on the SiC foam tray.

In order to reflect the pore diameter on the SiC foam tray faithfully, x-ray 3-D imaging techniques is used to reconstruct the surface structure of the SiC foam monolithic tray. The tested SiC foam is 5 and 5 cm in length and width. The pore size is measured and the distribution of pore size is shown in Figure 3. The average pore size calculated is equal to 3.55 mm. As shown in Figure 3, the pore size on the surface of plate is not of uniform size. The pore diameter mainly concentrates around the 3–4 mm diameter, and there is some smaller pore around 2-mm diameter.

Results and Discussions

Influence of the structure for the SiC foam monolithic tray on the gas holdup distribution

Figure 4 shows the distribution of the local gas holdup on the SiC foam trays with different thickness. The test trays are all in 3-mm pore diameter, the differences among trays with 4-, 8-, and 12-mm thick are discussed. On the tray with 4- and 8-mm thickness, the number of test points with gas holdup less than 10% is about 25–30, which illustrates that there is hardly any bubble formation on these points. Furthermore, on the 4-mm-thick tray, there exists more than 10 points with the gas holdup larger than 90%, which reflects that the bubble formation concentrates on these positions. Compared with the trays with 4- and 8-mm-thick tray, the number of points with the gas holdup less than 10% is about 7, and there is no point with the gas holdup larger than 90% for the tray with 12-mm thick. The results illustrates that the distribution of gas holdup is more uniform for the tray with 12-mm thick.

The pressure drop for the SiC foam tray (ΔP_{SiC}) is directly proportional to thickness of SiC foam. The measured dry

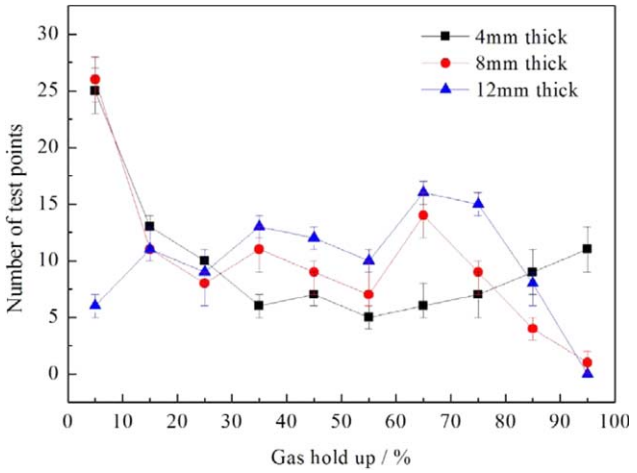

Figure 4. The influence of the tray thickness on the distribution of the gas holdup for the SiC foam monolithic tray with 3-mm pore size.

$F = 1.0\ \mathrm{kg^{1/2} \cdot m^{-1/2} \cdot s^{-1}}$, $L = 2.86\mathrm{m^2 \cdot h^{-1}}$, $H_w = 30$ mm. [Color figure can be viewed in the online issue, which is available at wileyonlinelibrary.com.]

pressure drop of the SiC foam tray with 3-mm pore size for thickness of 12, 8, and 4 mm is, respectively, 85, 45, and 23 Pa. The dry pressure drop is measured by the U-type manometer when the $F = 1.0\ \mathrm{kg^{1/2} \cdot m^{-1/2} \cdot s^{-1}}$. As discussed in the process model of the gas distribution, the dry pressure drop of SiC foam (ΔP_{SiC}) decides the impetus pressure under the tray in the Stage III. Therefore, the increasing of ΔP_{SiC} will make bubbles formation on more points of the tray.

Figure 5 shows the distribution of the local gas holdup on the SiC foam trays with different pore sizes. The tray with 4-mm pore size and 4-mm thick is not in our consideration, because the weeping rate is equal to 14% when the F-factor is $1.0\ \mathrm{kg^{1/2} \cdot m^{-1/2} \cdot s^{-1}}$, which is unable to cooperate properly.[1] As shown in Figure 5, on the 8-mm-thick tray, the tray with 4-mm pore size has an unequal gas distribution. About 55 test points have a gas holdup less than 10%, which reflects that the half of the tray has no bubble formation. The tray with 3-mm pore size performs better compared with the 4-mm pore size, the points with no bubble formation decrease to 25. The tray with 2-mm pore size has best gas holdup distribution, almost all the test point, there exists bubble formation.

As deduced from the process model of the gas distribution in the Stage I, the surface tension becomes weak with the increasing of the pore size. On the tray with 4-mm pore size, the pore diameter is larger than the capillary length, water could easily flow into the porous of SiC and obstruct air channel. The obstruction channel cannot allow the air through unless the pressure under the tray is larger than the surface adhesive force (P_τ). As a result, the gas holdup distributes unequally on the SiC foam tray. Meanwhile, the measured dry pressure drop of SiC foam tray (ΔP_{SiC}) is, respectively, 77, 45, 31 Pa corresponding 2-, 3-, and 4-mm pore size for the 8-mm-thick tray. In Stage III of the process model, large pressure drop (ΔP_{SiC}) will lead more points become active and lead an equal gas distribution.

Figure 5b shows the distribution of the gas holdup on the SiC foam tray with 12-mm thickness. The tendency of figure is similar to previous one, the tray with 4-mm pore size does not perform well, but the 3-mm pore size tray is analogous to the 2-mm pore size, which is influenced largely by the increase of thickness of SiC foam. Compared with 8-mm-thick tray, 12-mm-thick tray causes higher pressure drop (ΔP_{SiC}), the pressure drop of the trays with 2-, 3-, 4-mm pore size is, respectively, 116, 85, 50 Pa. Deducing from the process model, the pressure drop of the tray with 3-mm pore size and 12-mm thick is high enough to lead an equal gas distribution.

Influence of F-factor on the gas holdup distribution

In the process of bubble formation, the gas volume flux acts a significant role. Figure 6 shows that the distribution of the gas holdup on the foam tray with three pore size at 1.0 and $0.13\ \mathrm{kg^{1/2} \cdot m^{-1/2} \cdot s^{-1}}$. As shown in three Figures, the gas holdup on the SiC foam tray is better distributed with $F = 1.0\ \mathrm{kg^{1/2} \cdot m^{-1/2} \cdot s^{-1}}$ compared with the $F = 0.13\ \mathrm{kg^{1/2} \cdot m^{-1/2} \cdot s^{-1}}$. In smaller gas volume flux, the distribution of the gas phase on the foam tray maintains a relatively lower level, about 80% of test points have gas holdup

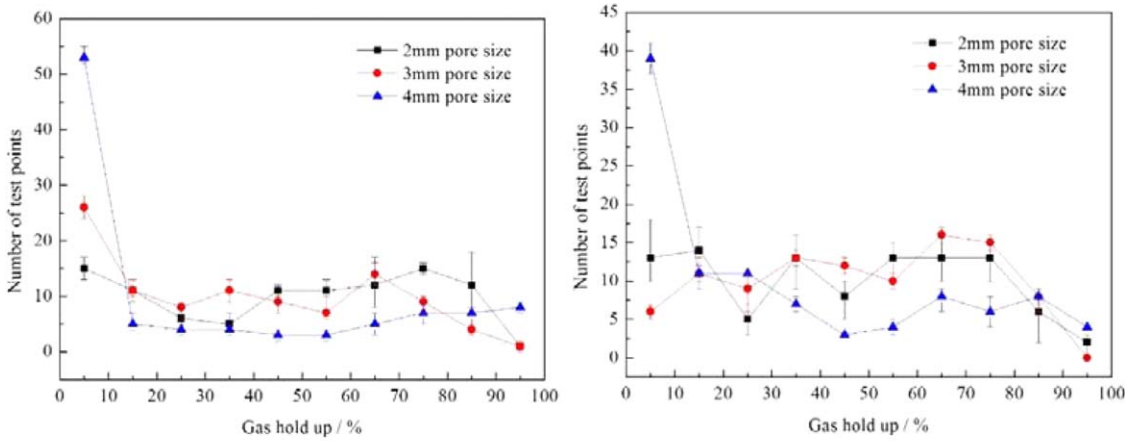

Figure 5. The influence of the pore size on the distribution of the gas holdup for the SiC foam tray with (a) 8 mm thickness and (b) 12 mm thickness.

$F = 1.0\ \mathrm{kg^{1/2} \cdot m^{-1/2} \cdot s^{-1}}$, $L = 2.86\mathrm{m^2 \cdot h^{-1}}$, $H_w = 30$ mm. [Color figure can be viewed in the online issue, which is available at wileyonlinelibrary.com.]

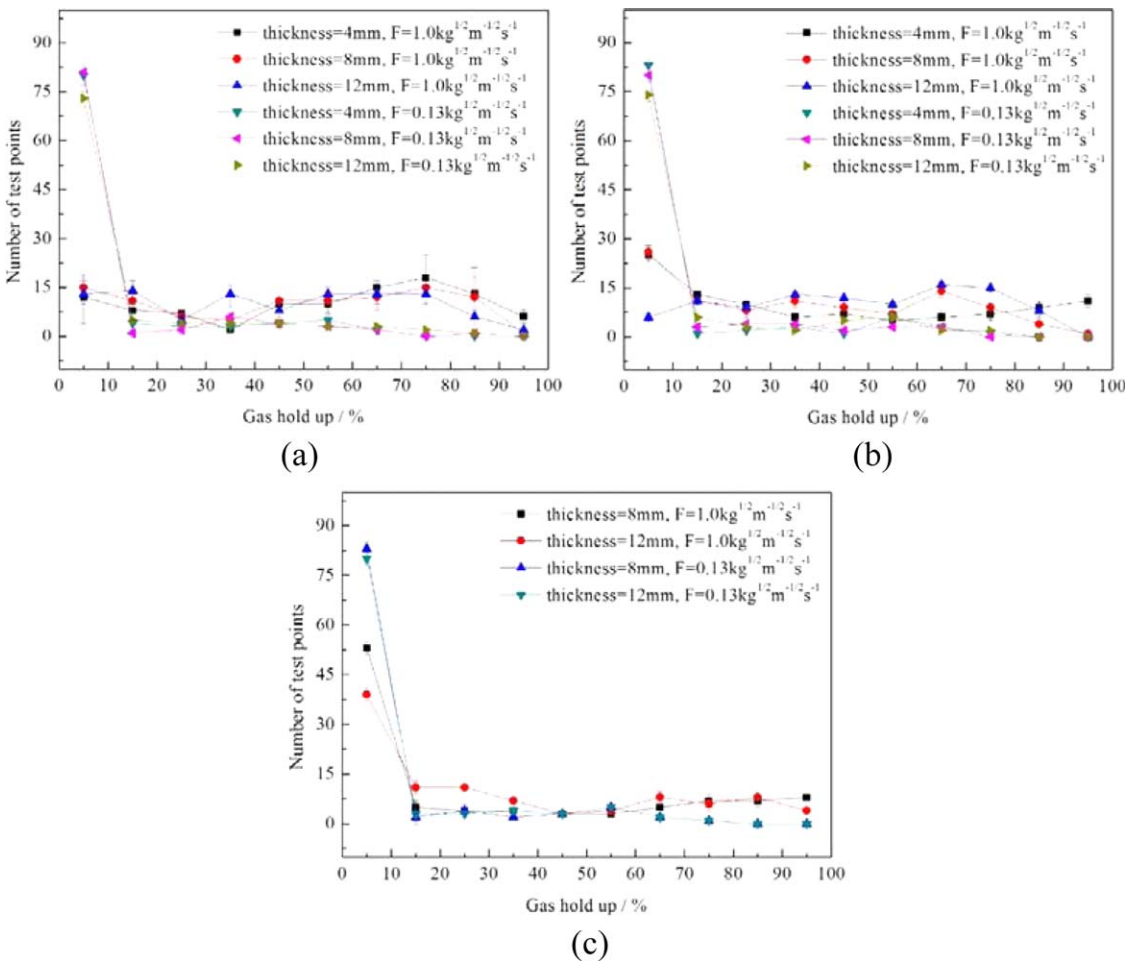

Figure 6. The influence of *F*-factor on the distribution of the gas holdup.

(a) Foam tray with 2-mm pore size; (b) foam tray with 3-mm pore size; (c) foam tray with 4-mm pore size. ($F = 1.0\ \mathrm{kg^{1/2} \cdot m^{-1/2} \cdot s^{-1}}$, $F = 0.13\ \mathrm{kg^{1/2} \cdot m^{-1/2} \cdot s^{-1}}$.) [Color figure can be viewed in the online issue, which is available at wileyonlinelibrary.com.]

less than 10%. The pressure drop of the foam tray stays at a corresponding low value when the *F*-factor is 0.13 $\mathrm{kg^{1/2} \cdot m^{-1/2} \cdot s^{-1}}$. Therefore, the bubble formation could only take form in the positions where the residence are weak as discussed in the Stage II of the process model. With the increasing of gas volume flux, the pressure drop of the foam tray increases to a corresponding higher value. The driving force is large enough to overcome the residence of the pore in more points, which results in the better gas-phase distribution. Meanwhile, the increase of bubbling points can be revealed by the wet pressure drop of the SiC foam tray, which will be discussed below.

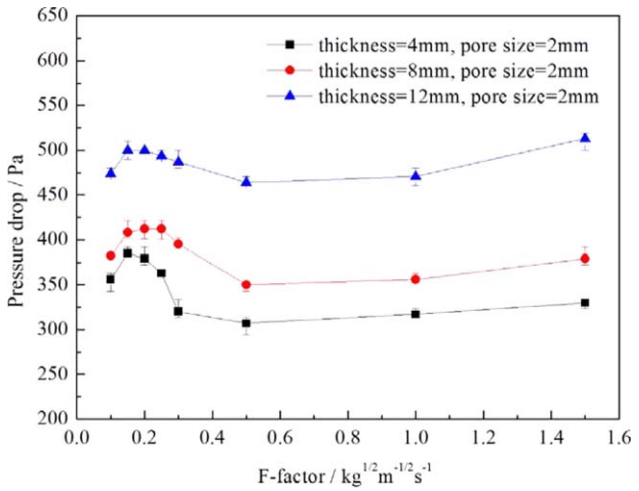

Figure 7. The wet pressure drop per tray of various foam tray as a function of *F*-factor at liquid flow 2.86 $\mathrm{m^2 \cdot h^{-1}}$.

[Color figure can be viewed in the online issue, which is available at wileyonlinelibrary.com.]

As shown in Figure 7, the changes of the wet pressure drop present an S-shaped curve with the increasing of *F*-factor. When *F*-factor arranges from 0.1 to 0.2 $\mathrm{kg^{1/2} \cdot m^{-1/2} \cdot s^{-1}}$, the wet pressure drop increases with the *F*-factor increasing. This is because the bubbling points are lack, the flow rate of the gas on single orifice is big, and the vortex flow is violent in a single orifice. When *F*-factor arranges from 0.2 to 0.5 $\mathrm{kg^{1/2} \cdot m^{-1/2} \cdot s^{-1}}$, the wet pressure drop decreases with the *F*-factor increasing. Because more bubbling points take form at the higher pressure drop of the foam tray. The increasing of bubbling points decrease the flow rate of the gas on the orifice, which lead to less vortex flow in a single orifice. When *F*-factor is larger than 0.5 $\mathrm{kg^{1/2} \cdot m^{-1/2} \cdot s^{-1}}$, the wet pressure drop increases continuously with the *F*-factor increase. This result is attributed to almost all of the hole has been opened by the highly gas flow rate that results in a higher pressure drop of the foam monolithic tray. With the increase of the gas rate, there is no holes continues can be open. So the pressure drop of the foam tray increases with the *F*-factor increasing when the *F*-factor larger than 0.5 $\mathrm{kg^{1/2} \cdot m^{-1/2} \cdot s^{-1}}$.

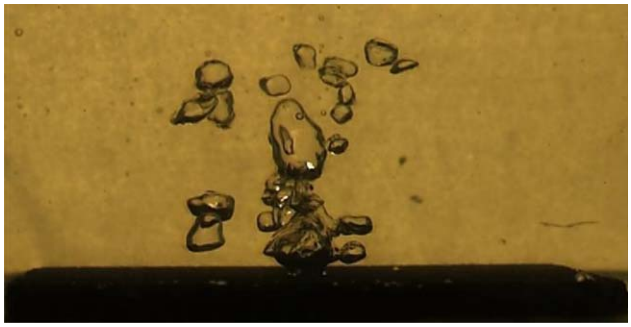

Figure 8. Bubbles generation on the SiC foam tray captured by high-speed camera.

[Color figure can be viewed in the online issue, which is available at wileyonlinelibrary.com.]

Characteristics of the bubble size distribution

The photograph captured by high-speed camera is shown in Figure 8, hundreds of photos are chosen to calculate the bubble diameter and get the bubble size distribution. There were a lot of researches about bubble formation on single orifice, the calculation of bubble size has not formed a unified conclusion, but most of researchers agreed that the bubble size was proportional to the gas flow rate and orifice diameter.[27] For the bubble formation on the SiC foam tray, we infer that the bubble size is also proportional to the gas flow rate and orifice diameter. In the following contest, as shown in Figure 9, the impacts of pore size and thickness to the bubble size distribution are presented, and the Sauter mean diameter ($D_{32}=\sum d_i^3/\sum d_i^2$) with standard deviation are addressed.

From Figure 9, for the test trays with the same thickness, the small pore size leads a narrow probability distribution and concentrates on small bubble size compared with the large pore size. As would be expected, the bubbles size on the tray increase with the pore size of the foam tray increasing. The changes of mean diameter also shows that with the increase of pore size, the D_{32} increases, and the standard deviation increases with the pore size which reflects that the discreteness with different pore size.

For the test trays with the same pore size, the thicker tray leads a narrow probability distribution and concentrates on small bubble size compared with the thin tray. Compare the D_{32} and standard deviation between different thickness, it is obvious that the mean diameter and standard deviation decrease with the increase of thickness. This suggests that the bubbles size on the tray decrease with the thick of the foam tray increasing. We can know from Figure 8 that two more

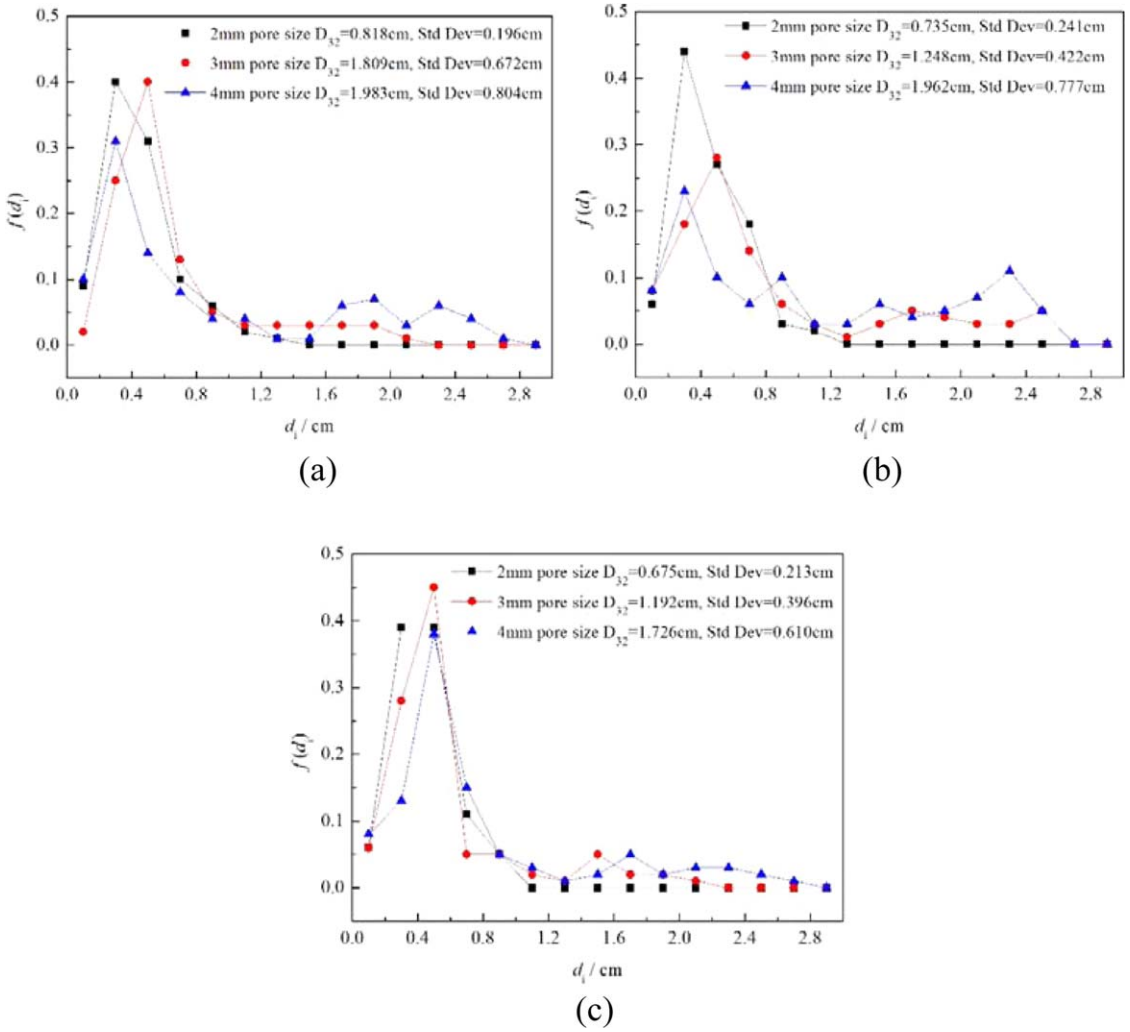

Figure 9. The influence of the pore size and tray thickness on the bubble size distribution.

(a) Foam tray with 4-mm thickness; (b) foam tray with 8-mm thickness; and (c) foam tray with 12-mm thickness. [Color figure can be viewed in the online issue, which is available at wileyonlinelibrary.com.]

bubbling points exist after the gas flow through one orifice under the SiC foam tray, the enumerated tray is 12-mm thick with 2-mm pore size.

Conclusions

In this article, a three-step model is put forward to describe the process of gas distribution on the SiC foam trays. The gas distribution performance of SiC foam trays is study in air-water system, at ambient temperature and pressure conditions. The distribution of local gas holdup is tested at $F = 1.0\ \mathrm{kg^{1/2} \cdot m^{-1/2} \cdot s^{-1}}$, $L = 2.86\ \mathrm{m^2 \cdot h^{-1}}$, $H_w = 22$ mm; and the bubble size distribution is studied on the single orifice. The characteristics of compounds have influence to the gas distribution, due to the capillary length changes with surface tension and density. Lower surface tension could only maintain the stability at small pore size, which means that the compounds with lower surface tension may match smaller pore size to have evenly gas distribution.

The pore size of SiC foam is the critical factor, smaller pore size will lead easier bubble formation and larger pressure drop. The thickness of SiC foam is also an important factor, the thicker tray will lead larger pressure drop. From the process model of gas distribution, large pressure drop will lead the gas equidistribution. Therefore, the SiC foam tray with small pore size and bigger thickness will have better gas distribution performance.

Acknowledgments

The authors are grateful for the financial support form National Natural Science Foundation of China (Nos. 21176172, 21336007), National High Technology Research and Development Program of China (No. 2015AA03A602), and they gratefully acknowledge the Institute of Metal Research of CAS for providing the SiC foam materials.

Notation

Roman letters

E_{OC} = overall column efficiency
F = gas F-factor through superficial area of tray, $\mathrm{kg^{1/2} \cdot m^{-1/2} \cdot s^{-1}}$
L = liquid weir loading, $\mathrm{m^2 \cdot h^{-1}}$
H_w = height of the overflow weir, mm
ΔP_{SiC} = pressure drop of SiC foam, Pa
P_c = capillary pressure, Pa
P_τ = pressure drop caused by the surface adhesive force, Pa
d = diameter of the pore size, mm
I_σ = capillary length, mm
d_i = diameter of bubble, cm

Greek letters

σ = surface tension coefficient, N/m
θ = contact angle, °

Literature Cited

1. Li XG, Liu DX, Xu SM, Li H. CFD simulation of hydrodynamics of valve tray. *Chem Eng Process*. 2009;48(1):145–151.
2. Zarei T, Rahimi R, Zarei A, Zivdar M. Hydrodynamic characteristic of Conical Cap tray: experimental studies on dry and total pressure drop, weeping and entrainment. *Chem Eng Process*. 2013;64:17–23.
3. Olujic Z, Jodecke M, Shilkin A, Schuch G, Kaibel B. Equipment improvement trends in distillation. *Chem Eng Process*. 2009;48(6): 1089–1104.
4. Soy U, Demir A, Caliskan F. Effect of bentonite addition on fabrication of reticulated porous SiC ceramics for liquid metal infiltration. *Ceram Int*. 2011;37(1):15–19.
5. Incera Garrido G, Kraushaar-Czarnetzki B. A general correlation for mass transfer in isotropic and anisotropic solid foams. *Chem Eng Sci*. 2010;65(6):2255–2257.
6. Patcas FC, Garrido GI, Kraushaar-Czarnetzki B. CO oxidation over structured carriers: a comparison of ceramic foams, honeycombs and beads. *Chem Eng Sci*. 2007;62(15):3984–3990.
7. Huu TT, Lacroix M, Huu CP, Schweich D, Edouard D. Towards a more realistic modeling of solid foam: use of the pentagonal dodecahedron geometry. *Chem Eng Sci* 2009;64(24):5131–5142.
8. Zeng J, Gao X, Li H, Tian C, Yang ZM, Zhang JS, Li XG. Hydrodynamic and mass transfer efficiency of SiC ceramic structured packing. *Mod Chem Ind*. 2012;32(10):70–73.
9. Leveque J, Rouzineau D, Prevost M, Meyer M. Hydrodynamic and mass transfer efficiency of ceramic foam packing applied to distillation. *Chem Eng Sci*. 2009;64(11):2607–2616.
10. Zhang LH, Liu XK, Li XG, Gao X, Sui H, Zhang JS, Yang ZM, Tian C, Li H. A novel SiC foam valve tray for distillation columns. *Chin J Chem Eng*. 2013;21(8):821–826.
11. Gao X, Li XG, Liu X, Li H, Yang ZM, Zhang JS. A novel potential application of SiC ceramic foam material to distillation: foam monolithic tray. *Chem Eng Sci*. 2015, DOI:10.1016/j.ces.2014.11.044.
12. Li XG, Liu X, Gao X, et al. Hydrodynamics behavior and mass transfer performance of novel SiC foam trays. *J Tianjin Univ*. 2014; 47(02):155–162.
13. Incera Garrido G, Patcas F, Lang S, Kraushaar-Czarnetzki B. Mass transfer and pressure drop in ceramic foams: a description for different pore sizes and porosities. *Chem Eng Sci*. 2008;63(21):5202–5217.
14. Lacroix M, Nguyen P, Schweich D, Pham Huu C, Savin-Poncet S, Edouard D. Pressure drop measurements and modeling on SiC foams. *Chem Eng Sci*. 2007;62(12):3259–3267.
15. Grosse J, Kind M. Hydrodynamics of ceramic sponges in countercurrent flow. *Ind Eng Chem Res*. 2011;50(8):4631–4640.
16. Munholand L, Soucy G. Comparison of four conductive needle probe designs for determination of bubble velocity and local gas holdup. *Rev Sci Instrum*. 2005;76(9):095101.
17. Dietrich N, Mayoufi N, Poncin S, Midoux N, Li HZ. Bubble formation at an orifice: a multiscale investigation. *Chem Eng Sci*. 2013;92:118–125.
18. Polli M, Di Stanislao M, Bagatin R, Abu Bakr E, Masi M. Bubble size distribution in the sparger region of bubble columns. *Chem Eng Sci*. 2002;57(1):197–205.
19. Hu B, Yang H-M, Hewitt GF. Measurement of bubble size distribution using a flying optical probe technique: application in the highly turbulent region above a distillation plate. *Chem Eng Sci*. 2007; 62(10):2652–2662.
20. Zhang WH, Li XG. Local gas holdup profiles in an internal-loop airlift reactor. *CIESC J*. 2010;61(05):1118–1122.
21. Zhang WH, Li XG. Origin of pressure fluctuations in an internal-loop airlift reactor and its application in flow regime detection. *Chem Eng Sci*. 2009; 64:1009–1018.
22. Buwa VV, Ranade VV. Dynamics of gas-liquid flow in a rectangular bubble column: experiments and single/multi-group CFD simulations. *Chem Eng Sci*. 2002;57(22-23):4715–4736.
23. Camarasa E, Vial C, Poncin S, Wild G, Midoux N, Bouillard J. Influence of coalescence behaviour of the liquid and of gas sparging on hydrodynamics and bubble characteristics in a bubble column. *Chem Eng Process: Process Intensif*. 1999;38(4):329–344.
24. Polli M, Di Stanislao M, Bagatin R, Bakr EA, Masi M. Bubble size distribution in the sparger region of bubble columns. *Chem Eng Sci*. 2002;57(1):197–205.
25. Kasimsetty SK. *Theoretical Modeling and Correlational Analysis of Single Bubble Dynamics from Submerged Orifices in Liquid Pools*, University of Cincinnati; 2008.
26. Kafka FY, Dussan E. On the interpretation of dynamic contact angles in capillaries. *J Fluid Mech*. 1979;95(03):539–565.
27. Davidson L, Amick EH. Formation of gas bubbles at horizontal orifices. *AIChE J*. 1956;2(3):337–342.

Manuscript received Feb. 12, 2015, and revision received May 1, 2015.